Altering the Stability of Surface Plastic Flow via Mechanochemical Effects

Anirudh Udupa,[1,*,†] Tatsuya Sugihara,[2,†] Koushik Viswanathan,[1] and Srinivasan Chandrasekar[1]

[1] *Center for Materials Processing and Tribology, Purdue University, West Lafayette, Indiana 47907-2023, USA*

[2] *Department of Mechanical Engineering, Osaka University, Suita, Osaka 565-0871, Japan*

(Received 10 July 2018; revised manuscript received 17 October 2018; published 10 January 2019)

We demonstrate a link between surface plastic flow and the ambient chemical environment—a mechanochemical effect—in large-strain deformation of metals, using high-speed *in situ* observations. This link, which is different from known mechanochemical effects, is studied using aluminum and an alcohol environment. Three distinct flow modes—sinuous, laminar, and segmented—occur, depending on the action of alcohol on the metal surface. Two transitions, one from sinuous to laminar and the other from sinuous to segmented flow, are demonstrated. In both cases, the final flow modes are characterized by smaller deformation forces (an order of magnitude) as well as a much improved quality of the final surface. The action of the chemical medium itself is coupled to the flow mode, distinguishing it from other mechanochemical effects that have previously been reported. The effect appears to be replicable to different degrees in other metal systems such as copper, iron, stainless steels, and nickel. Based on the observations, a schematic stability phase diagram for plastic flow is proposed. Implications of the results for enhancing the performance of cutting and surface-deformation processes for soft and highly strain-hardening metals are discussed.

DOI: 10.1103/PhysRevApplied.11.014021

I. INTRODUCTION

It has long been appreciated that the nature of mesoscale plastic flow in metals is determined by considerations of stability [1–4]. The prime and most often cited example in this regard is, perhaps, the change from uniform homogeneous plastic flow to localized deformation in the form of shear bands [1,5]. This example of a homogeneous to nonhomogeneous flow transition occurs in an array of material systems, from rocks on the geological scale [6] to structural metals on the mesoscale [5,7,8] and to glasses on the nanoscale [9]. However, the fact that other such transitions may also exist, particularly in large-strain deformation, resulting in flows that have hitherto been poorly understood, is only now beginning to be appreciated [10–12]. It is quite natural to expect that these transitions can also be explained in terms of changes in stability, thereby predicting the characteristics of the resulting flow.

The nature of plastic flow is particularly important in large-strain-deformation processes at or near free surfaces, i.e., unconstrained deformation. The proximity of the free surface to the deformation zone provides an additional degree of freedom for flow evolution, thereby being potentially conducive to spawning a rich variety of nonhomogeneous flows. A common feature of these deformation processes is use of intense shear to effect changes in shape, microstructure, and surface properties. Such processes are ubiquitous in materials processing and manufacturing, encompassing, to name a few, cutting, abrasion, and sliding [13,14].

A related, but well-known, fact is that surface plastic deformation is intimately linked to the environment to which the free surface is exposed to during deformation, as well as the presence of thin surface layers (e.g., oxide films) [15]. For instance, the exposure of the surface of certain, otherwise highly ductile, metals to suitable chemical media is known to cause severe embrittlement, e.g., stress-corrosion cracking and hydrogen and/or liquid metal embrittlement [16–18]. These processes are also governed by stability considerations, such as the competition between continued plastic flow and fracture [19–21].

Naturally, given the important consequences of surface-flow modes and the potentially central role of flow stability in determining them, it is of interest to examine the following question: Can we induce transitions from one flow mode to another, by utilizing a suitable chemical environment? This question is also pertinent from a practical point of view, because—driven by implications for machining, deformation processing, and tribology—there is much interest in controlling specific flow modes in surface plasticity [22,23]. In manufacturing, the flow mode determines process performance indices such as forces, energy consumption, and surface quality. Likewise, wear processes

*audupa@purdue.edu

†A.U. and T.S. contributed equally to this work.

are closely linked with the occurrence of nonhomogeneous flow modes near free surfaces [24–27].

In the course of an examination of this question, we discover that metals can exhibit widely different flow modes in the presence of suitable chemical media [10,28]—a subclass of phenomena termed mechanochemical effects [22,29]. Notably, a material-independent mechanochemical effect is found in the cutting of ductile and highly strain-hardening metals [28]. By using a chemical medium that physically adheres to the metal's surface, the type of plastic flow is fundamentally altered. Based on surface energetics considerations, this change is shown to resemble a local ductile-to-brittle transition.

The present paper describes a different, yet complementary, mechanochemical effect that is material- and chemical-medium specific. We use a specially designed system—aluminum plastically deformed to large strains in an alcohol environment—that demonstrates the intricate coupling between surface-plastic-flow modes, both homogeneous and nonhomogeneous, and the surrounding chemical environment. The two key features of our system that help to unearth this coupling are the ductility of Al and its chemical reactivity with alcohols. The observations provide a strong basis for the hypothesis that the plastic-deformation mode operative at surfaces is determined by flow-stability considerations. They also suggest possibilities for beneficially utilizing these effects in cutting and deformation processing of metals. It is of interest to note here that while the present study is focused on metals, mechanochemical effects involving solid- and/or liquid-state chemical reactions have been exploited commercially in nonmetallic systems, e.g., chemomechanical polishing of Si and ceramics [30–32].

The manuscript is organized as follows. Section II provides background information on surface-plastic-flow modes and the uniqueness of the aluminum-alcohol system. The details of the experimental system are discussed in Sec. III, followed by the results (Sec. IV). We explain the results within the framework of flow stability and propose a phase diagram for evaluating stability in the presence of chemical media (Sec. V). This section also discusses some implications for manufacturing processes with metals and related avenues for future work. Concluding remarks are presented in Sec. VI.

II. BACKGROUND

The prototypical mode of plastic flow in large-strain deformation is one of steady homogeneous strain, typically with smoothly varying and time-independent strains. In addition, three other flow modes have been identified—one unknown until recently—each with their own distinct features.

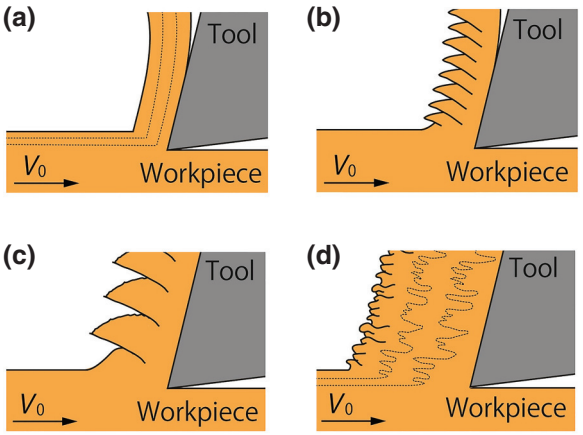

FIG. 1. A schematic of the four principal plastic-flow modes and corresponding chip morphologies in simple-shear deformation of metals by cutting: (a) laminar flow; (b) shear-band flow; (c) segmented flow; and (d) sinuous flow. The flow modes may be characterized by the overlaid streakline pattern shown here for modes (a) and (d).

A. Four distinct surface-plastic-flow modes

To best illustrate these flow modes and their features, a prototypical large-strain, simple-shear-deformation geometry is presented in Fig. 1, which schematically depicts all four flow modes. This configuration resembles plane-strain cutting and involves the imposition of simple shear on a moving workpiece using a sharp wedge-shaped tool. The shearing process removes a thin layer of material from the workpiece, the chip (see Fig. 1). The four flow modes result in distinct morphologies in the chip, a fact that has only recently begun to be appreciated based on combined *in situ* and *ex situ* analyses [11,12,33], even though chip morphologies themselves have been studied for a long time [5,13,34–36]. The four modes are as follows: (1) steady homogeneous deformation, henceforth referred to as laminar flow [Fig. 1(a)]; (2) shear-band flow, with periodic deformation restricted to very narrow zones [1,3,5], as in Fig. 1(b); (3) segmented flow, characterized by nonuniform deformation and periodic fracture, as in Fig. 1(c); and (4) the more recently uncovered sinuous flow, typified by surface (plastic) buckling, material folding, and highly nonhomogeneous straining [Fig. 1(d)] [10,11]. The latter three modes, being nonhomogeneous and unsteady, will be referred to as nonlaminar flow modes. *In situ* and *ex situ* observations [12] have established that these different flow modes result in chips with characteristic morphologies (signatures) (see Fig. 1). Similar flow modes and wear-particle morphologies have also been observed in sliding, another well-known, large-strain deformation process [27].

B. The role of stability

This rich diversity of flow modes in cutting and sliding is a direct consequence of the presence of the free

surface and is quite distinct from the more limited flow patterns typical of constrained deformation processes such as bulk metal forming [37]. Which of these flow modes actually occurs in a certain situation is determined by stability criteria, including considerations of surface plastic buckling [33] and crack growth from free-surface flaws [15,38] as well as the material's inherent propensity to exhibit flow localization [3]. In manufacturing and materials processing, a large body of evidence exists to show that the flow mode and the stability of the flow are strongly influenced by the initial deformation state of the metal (e.g., annealed, prestrained) and the deformation geometry (e.g., the die angle) [13,37]. Furthermore, the presence of specific chemical environments is known to introduce additional constraints on flow stability, by promoting auxiliary processes such as crack nucleation and growth [22,23,39].

C. Aluminum and its reactivity with alcohols—a model system

The use of Al and alcohols as a model system for studying chemical environment effects on surface plastic flow has three primary advantages.

First, commercially pure aluminum, based on the initial deformation state of its surface, is known to demonstrate at least three of the four flow modes discussed in Fig. 1 [11,40]. Therefore, using this metal for studying large-strain deformation allows us, in principle, to probe the effect of a chemical environment on multiple flow modes within the same material system.

Second, fresh Al surfaces readily react with alcohols to form alkoxides, an important class of compounds characterized by aluminum—oxygen—carbon bonding [41]. Industrially, alkoxides such as isopropoxide and sec-butoxide are important for the production of ketones and aldehydes, where they are employed as reducing agents [42]. When a fresh Al surface reacts with isopropyl alcohol, the resulting aluminum isopropoxide formed is a white solid (melting point 118 °C), otherwise usually prepared by an elaborate synthesis method via the formation of an amalgam [43].

Third, alcohols and the resulting alkoxides can be effective lubricants [44–47]. The lubrication is claimed to be effected by a negative-ion-radical mechanism that changes the interface conditions during sliding [48].

Thus the Al-alcohol system offers much scope for altering the nature of the shear deformation at surfaces (e.g., Fig. 1), both via the formation of alkoxide layers to effect surface-energy changes and via lubricant films to change the friction at and near the deformation zones.

III. EXPERIMENTAL DETAILS

Large-strain deformation is imposed using the model framework of a workpiece sliding at constant velocity V_0 against a rigid wedge (a tool or die) (see Fig. 2). As the workpiece is pushed against the wedge or tool, a thin layer of material, of initial thickness h_0, is continuously deformed under simple shear and removed as a "chip" of thickness h_C, with a fresh surface created on the workpiece. The ratio $\lambda = h_C/h_0$ is typically between 2 and 20, depending on the underlying flow mode [11,12,33,36]. This configuration, analogous to cutting, is well characterized in terms of loading and chip deformation [13]. For the experiments described in this manuscript, V_0 is fixed at 5 mm/s. The low speed ensures that thermal effects on the deformation are minimal: for these conditions, the temperature change is estimated to be $<5\,^{\circ}$C [13]. The undeformed chip thickness (h_0) value is set nominally at 50 μm in the experiments. However, due to compliances in the tool and work-holding system, it is difficult to achieve this set value exactly. In practice, we use iterative adjustment of the h_0 setting to get an actual value that is close to the targeted value. The exact h_0 in the experiments is measured both from the images and by utilizing a dial indicator; these values are 55, 49, and 53 μm for the dry-cutting, isopropyl-alcohol- (IPA-)cutting, and alkoxide-cutting experiments, respectively.

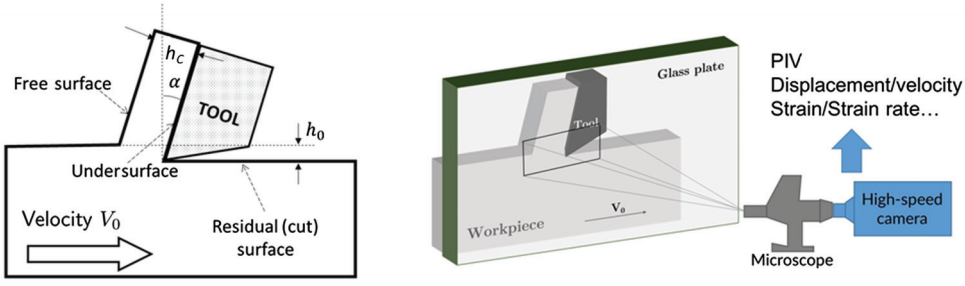

FIG. 2. A schematic of the plane-strain cutting used to impose simple-shear deformation in the chip and the high-speed imaging configuration used to characterize the flow patterns. Left, the notation defining the deformation geometry (α, h_0, h_C) and various surfaces of the workpiece and the chip (the free surface, the undersurface, and the cut surface). Right, the deformation zone is observed *in situ* to obtain quantitative flow-field information at high resolution.

A. Workpiece and tool properties

The tool is made of a commercial-grade WC-Co alloy, with a cutting-edge width of 2.3 mm (equal to the chip width), an edge radius of <5 μm, and a rake angle of $\alpha = 10^\circ$ (Fig. 2). The workpiece is commercially pure Al (Al 1100, dimensions—length 75 mm $\times$ height 25 mm $\times$ width 6 mm). The workpiece is prepared in an initially annealed state, by heating in a furnace at 550 °C for 4 h and then furnace cooling to room temperature. The reason for using aluminum in the annealed condition is because in this state it is soft and ductile and exhibits unsteady sinuous via plastic buckling while cutting [33]. This enables the examination of unsteady and, potentially, multiple flow modes within the same material system.

B. The *in situ* characterization of the surface-plastic-flow modes

Plastic flow in the deformation zone during chip formation is recorded *in situ* using a high-speed CMOS camera (PCO dimax) coupled to a long-working-distance microscope objective (see Fig. 2, right). The deformation zone is illuminated using a 150-W halogen lamp. A glass block is clamped against the side face of the workpiece to constrain the deformation to remain as plane strain (see Fig. 2). Images are captured at 500 frames/s and a spatial resolution of 1.4 μm per pixel. The image sequences are analyzed using a digital-image-correlation technique—particle image velocimetry (PIV)—to obtain quantitative details of the flow, such as the effective (von Mises) strain and strain-rate fields, and the flow-line patterns [10]. These data enable detailed mapping of the underlying surface-plastic-flow modes.

Concurrently, forces on the tool, both parallel (cutting force F_c) and perpendicular (thrust force F_t) to V_0, are recorded using a mounted piezoelectric dynamometer (Kistler 9272, natural frequency approximately 2 kHz). The cutting force F_c is the primary contributor to the deformation energy and/or power, since it is oriented parallel to V_0 [13]. From these components, the resultant force is obtained, as well as the force components parallel (F_f) and perpendicular (F_n) to the tool face in contact with the chip. Since the actual h_0 values are slightly different for each of the three experimental conditions (dry, IPA, and alkoxide), the forces are normalized by dividing by h_0 to obtain specific force values ($\bar{F}_c = F_c/h_0$, $\bar{F}_t = F_t/h_0$) for each of the conditions. The specific force values and specific energy are used to characterize and analyze the energy dissipation corresponding to the three conditions (flow modes).

The topography of the cut (residual) surface in the wake of the tool is characterized using an optical profilometer (Zygo NewView 8300) to obtain surface roughness data and details of any defects, such as tears and cracks.

C. The role of the chemical environment

A series of cutting experiments is carried out within the framework of Fig. 2 to examine how the chemical environment in the vicinity of the workpiece and chip surface influences the plastic-flow modes. The reactivity of a freshly generated Al surface with isopropyl alcohol (henceforth IPA), coupled with the lack of reactivity between IPA and an oxide-covered Al surface, allows four different chemical conditions to be studied (see Fig. 3):

(1) *Dry cutting, Fig. 3(a)*: In the first series of experiments, the cutting is performed without the use of IPA or any other fluid.

(2) *IPA cutting, Fig. 3(b)*: In a second series of experiments, the tool-workpiece region is flooded with commercially available IPA. In this ambient condition, the tool-chip contact interface is altered due to the formation of a layer of aluminum isopropoxide (alkoxide) on the chip undersurface, facilitated by the freshly generated oxide-free Al surface. In the absence of such an oxide-free surface, this reaction between aluminum and IPA needs either the presence of a catalyst or high temperatures to overcome the natural oxide layer. Figure 3(b) indicates locations where alkoxide is formed as freshly exposed aluminum comes into contact with IPA. The alkoxide layer thus formed acts as a lubricating film at the tool-chip contact (see Sec. II).

(3) *Alkoxide cutting, Fig. 3(c)*: A third series of cutting experiments is performed by cutting without any IPA at all, but with an alkoxide film on the workpiece free surface, remote from the tool-chip contact zone. This film is formed as follows. The IPA cutting (above), besides altering the chip undersurface, leaves behind an alkoxide layer along the entire length of the residual (cut) surface [see Fig. 3(b)]. This is because the freshly generated and oxide-free cut surface, being highly reactive, forms an alkoxide film upon continuous exposure to the IPA. Now performing a second cutting pass over this newly created surface on the same workpiece (with identical values of h_0 and V_0) amounts to cutting a workpiece with a thin alkoxide film on its free surface. Since the residual strain on the workpiece surface after IPA cutting is small—$<$ 0.4 as estimated by PIV—the flow in the alkoxide cutting has found to be negligibly influenced by this residual strain. This is confirmed in multiple experiments. A discussion of residual strain effects on the cutting flow mode can be found in Ref. [11].

(4) *IPA + alkoxide cutting, Fig. 3(d)*: A fourth series of cutting experiments is performed wherein an alkoxide film is present on both the initial workpiece free surface as well as the chip undersurface. For this purpose, the cutting is done as in the alkoxide-cutting case, but with the tool-workpiece region flooded with IPA.

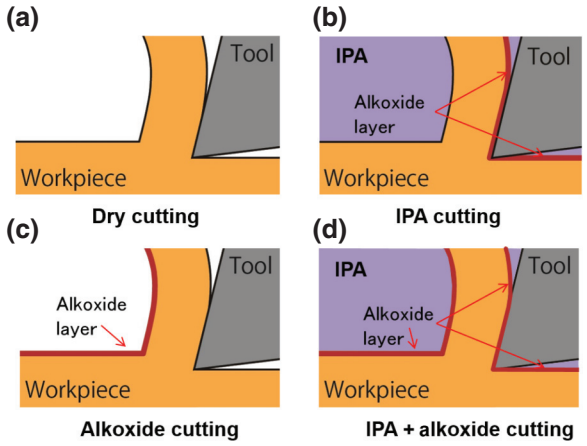

FIG. 3. Descriptions of the four different chemical ambient conditions used in cutting experiments with annealed Al. (a) Dry cutting: the cutting of annealed Al without the use of any medium. (b) IPA cutting: the cutting of annealed Al in a bath of IPA. As a consequence, the chip undersurface and the newly generated workpiece surface in the wake of the wedge tool are both directly exposed to the IPA soon after these surfaces are created. An alkoxide layer is formed on both the chip undersurface and the residual (cut) surface in the wake of the wedge. This provides a means of probing plastic-flow modes and flow stability by the action of IPA only along the chip undersurface. (c) Alkoxide cutting: the cutting of annealed Al, with an alkoxide layer on its free surface, without the use of any medium. This condition provides a means of probing the flow stability when only the initial workpiece surface is coated with an alkoxide layer. (d) IPA + alkoxide cutting: cutting with an alkoxide layer formed on both the free surface as well as the chip undersurface. This condition provides a means of probing the flow stability when there is an alkoxide layer on both surfaces.

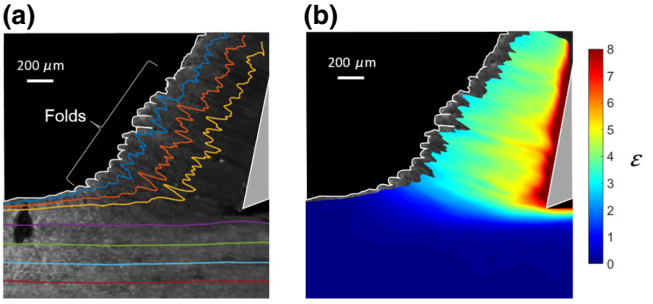

FIG. 4. The flow pattern and deformation in dry cutting. (a) An image from a high-speed sequence with superimposed streaklines from PIV. The highly wavy streaklines are characteristic of folding and sinuous flow. (b) The strain distribution is highly nonhomogeneous due to the folding. The ratio ($\lambda = h_C/h_0$) of the deformed to the undeformed chip thickness is 19, indicating extreme thickening of the chip and deformation. Note the mushroomlike structures on the free surface of the chip, which are typical of sinuous flow. $V_0 = 5$ mm/s and $h_0 = 55$ μm.

IV. RESULTS

The high-speed *in situ* observations capture flow modes in three different chemical environments, highlighting the influence of chemical media on the stability of the surface plastic flow. The results from these direct observations are complemented and/or reinforced by concurrent measurements of the force, the energy, and the quality of the cut surface.

A. Dry cutting

In the absence of any chemical (IPA), annealed Al deforms via sinuous flow under the chosen conditions; a typical chip is shown in Fig. 4. The chip is extremely thick, with the ratio $h_C/h_0 \simeq 19$, indicative of large underlying strains. Sinuous flow, a nonlaminar flow mode, is characterized by large-amplitude folding in the material, as revealed by the streaklines overlaid in Fig. 4(a). This type of flow is quite common in cutting of annealed and/or highly strain-hardening metals [10,11,33]. Figure 4(b) shows the effective (von Mises) strain in the chip, obtained from PIV. The chip strain distribution is quite nonhomogeneous, reflecting the repeated folding, and alternates between high (approximately 6) and low (<3) values. The folding also causes the free surface of the chip to have an irregular morphology with mushroomlike structures (Fig. 4). This morphology is typical of sinuous flow, as seen in other metals such as Cu and Fe.

Sinuous flow is initiated by plastic buckling of a thin surface layer ahead of the tool. Details of this flow development and its microstructure origins have been discussed in prior work [10,11,33], and may be summarized as follows. During sinuous flow, the material demonstrates repeated large-amplitude folding. Each folding event is initiated by the formation of a protuberance, or bump, on the free surface, resulting from plastic buckling. This bump formation is shown in Fig. 5, using the z component of the material velocity (V_Z), derived from PIV. V_Z in the chip (0.8 mm/s) is naturally greater than that in the workpiece (0 mm/s, V_0 horizontal). The zone in which the bump forms has a pronounced V_Z, in contrast to the surrounding material. The subsequent evolution of this bump into a fold is shown in the image sequence of Fig. 6. The initial bump is constrained between two material points (termed pinning points P_1 and P_2—see at the arrows) of minimal local curvature (frame 1). As the tool advances, these pinning points approach each other (frame 2) and the bump grows, evolving into a large-amplitude fold (frame 3). This process then repeats, with the folds stacking up closely on top of one another to form the thick chip ($\lambda = 19$). Each of the folds appears like a mushroom-shaped feature on the chip free surface [49] and the region between adjacent folds resembles a notch [28].

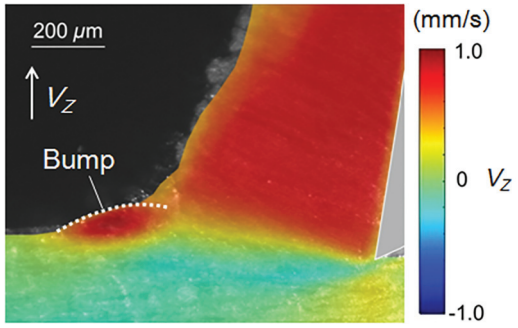

FIG. 5. The velocity distribution in the vertical direction (V_Z) in dry cutting. Bump formation is confirmed on the free surface by the sharp contrast between V_Z in the bump relative to the surrounding material.

B. IPA cutting

The large-amplitude folding and sinuous flow that accompany dry cutting result in very high cutting forces and a very thick chip. In sharp contrast, the chip formed in IPA cutting (cf., Fig. 3) is significantly thinner ($\lambda = h_C/h_0 \simeq 4.8$) than with dry cutting ($\lambda = 19$). Most strikingly, as seen in Fig. 7, the flow is homogeneous and laminar, as revealed by the smooth streaklines (see Movie 1). No folding is observable on the macroscale and the mushroomlike morphology (cf., Fig. 4) is also absent on the chip free surface. Additionally, the strain field in IPA cutting is homogenous throughout the chip [Fig. 7(b)], with much smaller maximum strain (approximately 3). The strain increases in a narrow region between the workpiece and chip, indicative of intense shear within a narrow zone (a "shear plane"), similar to the chip in Fig. 1(b). This laminar flow mode is what is usually seen in many large-strain shear-deformation conditions with moderately prestrained metals [34,50,51].

This transition in the flow from sinuous to laminar, with the same material and deformation geometry, is due to the lack of any buckling on the free surface in IPA cutting. Many alcohols, including IPA, are known to be effective lubricants for aluminum under conditions when a stable alkoxide layer is established on the Al surface [44].

In the present experiments, the existence of the alkoxide layer, on both the free surface and the chip undersurface, is detected using Fourier-transform infrared spectroscopy (FTIR). Specifically, absorbance peaks are detected in the 2840–3000 cm^{-1} and the 1720–1740 cm^{-1} ranges, indicating the presence of C—H and C = O bonds in the layer. It is expected that the thickness of the alkoxide layer so formed is approximately 15 nm [52]. In contrast, no alkoxide film is detected on the uncut workpiece free surface ahead of the tool due to the presence of the natural oxide layer on the Al. Thus, the IPA-cutting condition is ideal for examining the effect of a lubricant film (here, alkoxide) on the plastic-flow modes.

The importance of this alkoxide layer in lowering the tool-chip friction and cutting forces, thereby reducing the propensity for surface buckling and folding, is discussed in Sec. E.

C. Alkoxide cutting

When compared to dry cutting, alkoxide cutting [see Fig. 3(c)] also produces a much thinner chip ($\lambda = 6.7$, Fig. 8); this chip is only slightly thicker than in IPA cutting ($\lambda = 4.8$). Surprisingly, however, the flow mode by which this thin chip forms is fundamentally different from the laminar flow of IPA cutting and, of course, also from the sinuous flow of dry cutting. Figure 8(a) shows the streakline pattern and characteristic attributes of this flow mode—segmented flow—derived from the high-speed imaging, while Fig. 8(b) shows the corresponding strain field. The streaklines indicate the highly unsteady nature of the deformation, but their pattern is quite different from that in sinuous flow (cf., Fig. 6 and Movie 2). The chip strain distribution is highly nonhomogeneous [Fig. 8(b)], with a strain of approximately 2 for the most part of the chip, interspersed with regions of narrow width with much higher strain (7–8) near the cracks. Segmented flow has in the past been observed in cutting of metals of limited ductility, such as β-brass, hard steels, and highly prestrained metals [13]. The manifestation of this flow mode in annealed Al, which is at the other extreme of the ductility spectrum, is therefore a strong indication that its

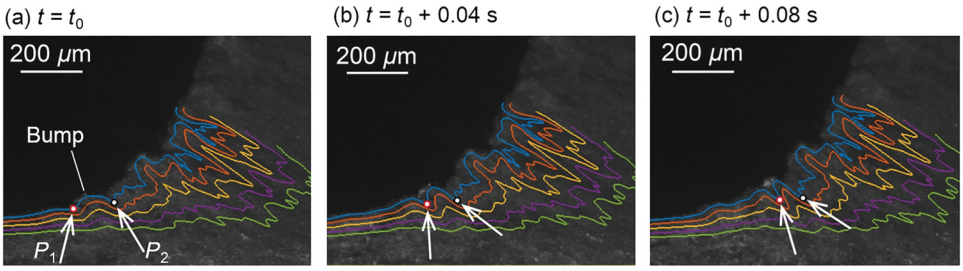

FIG. 6. The development of sinuous flow in dry cutting as captured by three frames from a high-speed sequence. (a) A bump is formed due to a plastic buckling instability between pinning points P_1 and P_2, ahead of the chip. The arrows track the positions of these pinning points in the frames. (b),(c) The bump grows in size (amplitude) and evolves into a fold, resulting in the wavy streaklines.

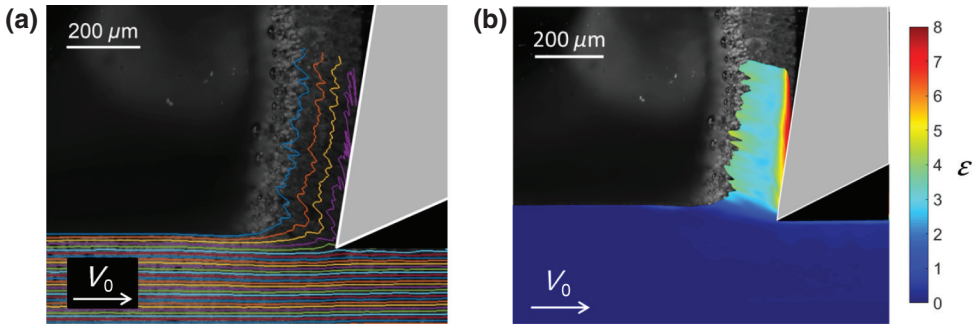

FIG. 7. The flow pattern and deformation in IPA cutting. (a) An image from a high-speed sequence with superimposed streaklines. The relatively smooth streaklines are indicative of laminar flow. (b) The strain distribution is now homogeneous. $\lambda = h_C/h_0$ is equal to 4.8, much smaller than in the sinuous-flow case. $V_0 = 5$ mm/s and $h_0 = 49$ μm.

surface has been "embrittled" by chemical reaction with the IPA. This is most likely because of alkoxide formation on the workpiece surface, facilitated by the specific conditions of the alkoxide-cutting experiment [Fig. 3(c)].

The embrittling effect of the alkoxide on the free surface is evident in the periodic cracks that initiate on the free surface, leading to individual segments. This process can be described using the three frames from a high-speed sequence shown in Fig. 9. A protuberance or bump, resembling the one initiating sinuous flow (Fig. 6), is formed, again by plastic buckling (see frame 1). Two neighboring material points in the bump region are highlighted in this frame (black and red dots). The evolution of a single segment can be inferred from the motion of these points, which eventually end up on opposite sides of a cracked surface. As the workpiece moves against the tool, the size of the bump does not increase to form a fold as in sinuous flow. Instead, a crack initiates at one of the pinning points and propagates from the workpiece surface (or free surface of the incipient chip) toward the tool tip. The propagation of this crack is reflected in the increased distance between the marked points in frame 2. The crack propagates to varying distances, depending on the cutting conditions (h_0, α, V_0), before it is arrested (frame 3). Subsequently, another plastic buckling event occurs, leading to a protuberance and cracking at a pinning point, and the process repeats. In other words, sinuous flow is disrupted in the incipient folding stage itself by recurring crack formation leading to segmented flow.

These *in situ* observations of the transition from sinuous flow to segmented flow (cf., Fig. 1) show that the presence of the alkoxide on the free surface of the chip increases the propensity for a crack to nucleate and propagate. The incipient folds, caused by the surface buckling, provide precursor defects such as notches, wherein the chemical action causes local crack nucleation via changes to the metal's surface energy. Thus, it is only when the free surface of the metal is chemically altered that the sinuous flow transitions to segmented flow. This "mechanochemical" action of the IPA via the alkoxide surface layer thus appears to be strongly coupled to the prevailing flow mode: incipient sinuous flow favors this action with segmentation ensuing, while laminar flow does not. This type of effect wherein the chemical action of the medium is coupled to the flow mode is quite different from previously reported mechanochemical effects in surface plasticity [19,20,39].

Given that the alkoxide layer can induce two different plastic-flow modes depending on which surface it is present on, a natural question is the following: What would be the flow mode when an alkoxide layer is present on both the free surface as well as on the chip undersurface? The answer to this question was obtained from the IPA +

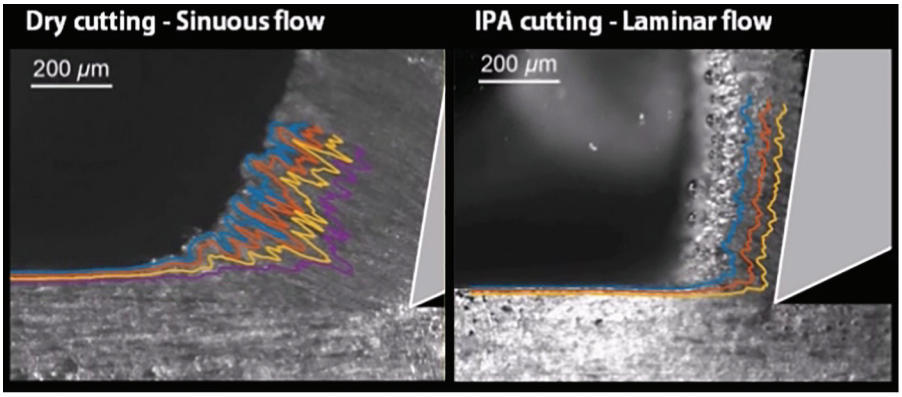

MOVIE 1. A comparison of dry cutting and IPA cutting. Dry cutting of annealed Al (left) results in sinuous flow, a thick chip, and a large cutting force. IPA cutting (right), on the other hand, results in a relatively smooth laminar flow, a thin chip, and a much smaller cutting force.

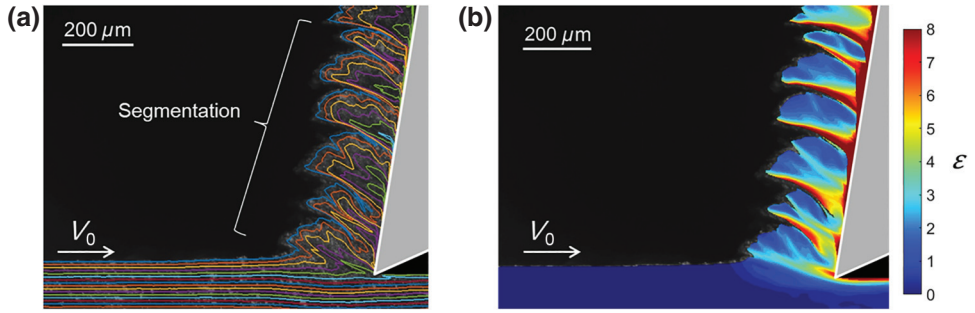

FIG. 8. The flow pattern and deformation in alkoxide cutting. (a) An image from a high-speed sequence with superimposed streaklines showing segmented flow. The alkoxide layer on the free surface of the chip or workpiece changes the flow mode from sinuous to segmented. Cracks nucleate periodically on the chip free surface and propagate toward the tool tip, giving rise to the segmented flow topology. (b) The (von Mises) strain is once again inhomogeneous, reflecting the nature of the deformation. $V_0 = 5$ mm/s and $h_0 = 53$ μm.

alkoxide cutting experiment [Fig. 3(d)]. In this experiment, the flow was laminar and the chip strain was homogenous, with $\lambda = 4.9$. In fact, this flow was essentially indistinguishable from the flow in IPA cutting in every respect. Hence, it is clear that whenever an alkoxide lubricant film is present at the tool-chip interface, laminar flow will always be the dominant flow mode. This is irrespective of whether an alkoxide layer is present on the chip free surface. Further implications of this result are discussed in Sec. V

D. Forces and energy consumption

The measured force components under all three chemical conditions are shown in Fig. 10. F_c [Fig. 10(a)] and F_t [Fig. 10(b)] represent the cutting (parallel to V_0) and thrust forces (normal to V_0) respectively, while $\bar{F}_c$ and $\bar{F}_t$ represent the forces normalized with respect to the actual undeformed chip thickness. In dry cutting, both components show a gradual increase to steady state, at which stage $\bar{F}_c \simeq 12N/\mu$m. This force value is quite high even though the material being cut is soft Al (23 HV)—a consequence of the large thickness change and deformation occurring in the workpiece material as it is converted into the chip [see Fig. 4 ($\lambda = 19$, strain 5–7)]. It is also worth noting that the friction force (the component along the tool face) F_f is 1.6 times F_n. If we define a friction coefficient (μ) for the tool-chip contact as the ratio F_f/F_n, then $\mu = 1.6$. In cutting of metals, this μ can assume values greater than unity [13]. It must be cautioned, however, that μ is more like a pseudo-friction-coefficient; for in cutting, its value is also influenced by the tool rake angle, rather than being determined completely by the chip and tool materials in contact, and the lubrication condition.

In laminar IPA cutting, both $\bar{F}_c$ and $\bar{F}_t$ are around 1.2 N/μm, values an order of magnitude smaller than those of the sinuous-flow mode of dry cutting (Fig. 10). Using F_c, the specific energy (the energy per unit volume of material removed) can be calculated as follows:

$$U = \frac{F_c V_0}{V_0 b h_0} = \frac{F_c}{b h_0}, \tag{1}$$

where b is the width of the cut. Since F_c is a direct measure of the specific energy in cutting, IPA cutting occurs with a much smaller energy consumption ($U_{\mathrm{IPA}} \sim 0.53$ J/mm^3) compared to the dry-cutting case ($U_{\mathrm{dry}} \sim 4.65$ J/mm^3). This is undoubtedly a consequence of the much smaller deformation imposed. Furthermore, unlike with sinuous flow, F_c and F_t reach their steady values much more

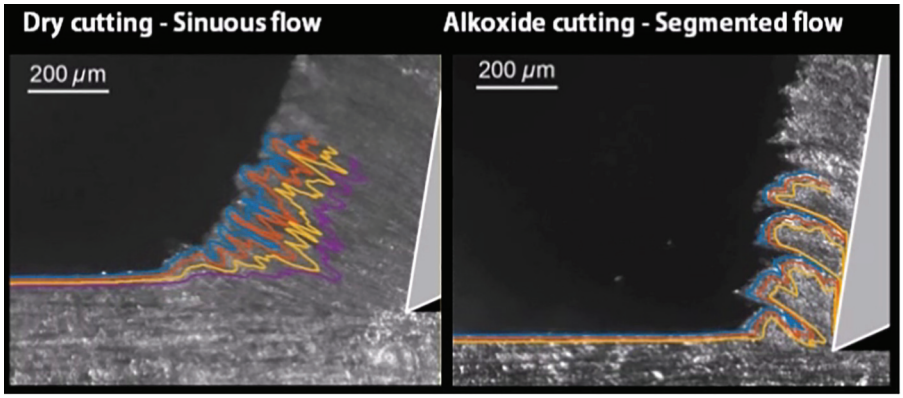

MOVIE 2. A comparison of dry cutting and alkoxide cutting. Dry cutting of annealed Al (left) results in sinuous flow, a thick chip, and a large cutting force. Alkoxide cutting (right), albeit still unlubricated, results in a segmentation-type flow, with cracks forming periodically and a much reduced cutting force.

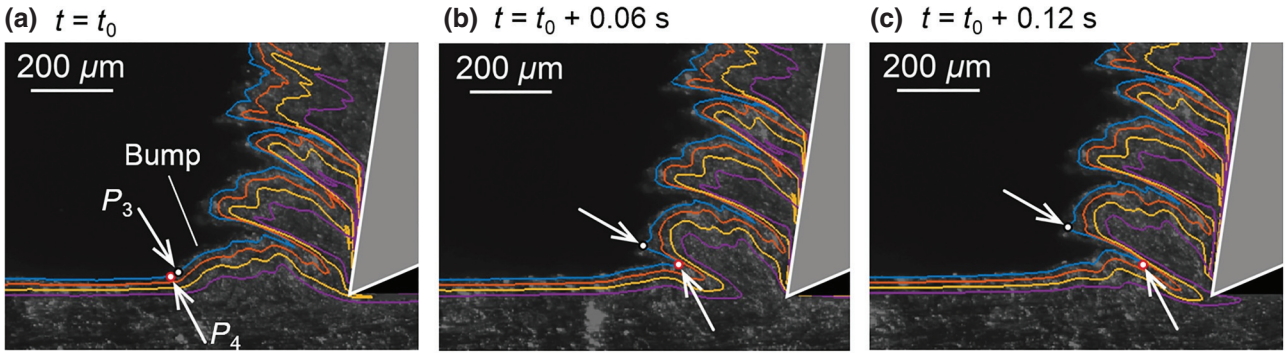

FIG. 9. The development of segmented flow in alkoxide cutting as captured by three frames from a high-speed sequence. (a) A bump is formed on the free surface, as in dry cutting. P_3 and P_4 show two neighboring (pinning) points in the bump region. (b) In contrast to dry cutting, the bump does not develop into a fold. Instead, a crack nucleates between the points P_3 and P_4, shown by the arrows. (c) The crack propagates toward the tool tip, as indicated by the increasing distance between these points.

quickly for the laminar flow mode. The tangential force, F_t, along the tool face in IPA cutting is also an order of magnitude smaller than in the dry-cutting case. Since this force is a measure of the frictional drag at the tool-chip contact, it shows that the IPA action at this contact has also reduced the frictional energy dissipation (secondary deformation) considerably. The change in friction can be inferred from the value of $\mu = 0.9$, which is significantly different from dry cutting ($\mu = 1.6$).

The case of IPA + alkoxide cutting is indistinguishable from the IPA-cutting case, not just from the flow mode but even from the specific forces. Even the value of $\mu = 0.8$ is very close to that for the IPA-cutting case. The observations strongly suggest that the friction force reduction in IPA cutting as well as the IPA + alkoxide cutting has stabilized the laminar flow mode *vis-à-vis* sinuous flow, by inhibiting the surface buckling.

In the case of alkoxide cutting, the forces and specific energy are again much smaller ($\bar{F}_c \sim 2$ N/μm, $U_{\text{alkoxide}} \sim 0.87$ J/mm^3) than in the sinuous-flow case, an almost 80% decrease (see Fig. 10). This large decrease is, at first sight, surprising since both conditions are essentially unlubricated, i.e., without any IPA access to the tool-chip interface. The unlubricated condition can be inferred from the value of $\mu = 1.5$, close to the dry-cutting case. However, the flow modes in these two cases are very different—segmented (alkoxide) versus sinuous (dry). The force reduction is due to the alkoxide layer on the initial workpiece surface triggering repeated fracture and segmented flow. The force decrease is, however, not as great as in the IPA-cutting case; likewise, the chip is also not as thin as in the laminar flow case (cf., Figs. 7 and 8). Furthermore, segmented flow cannot be inferred from the force trace alone, since this trace (Fig. 10) does not show any oscillations that might correspond to the periodic cracks in the chip.

E. The uniqueness of the Al-IPA system

The Al-IPA system is unique in that it can produce three of the four primary surface-flow modes in the same configuration, merely by varying the chemical environment. The underlying reason for this is the reactivity of an oxide-free Al surface with alcohols as well as the lubrication properties of the resulting alkoxide layer.

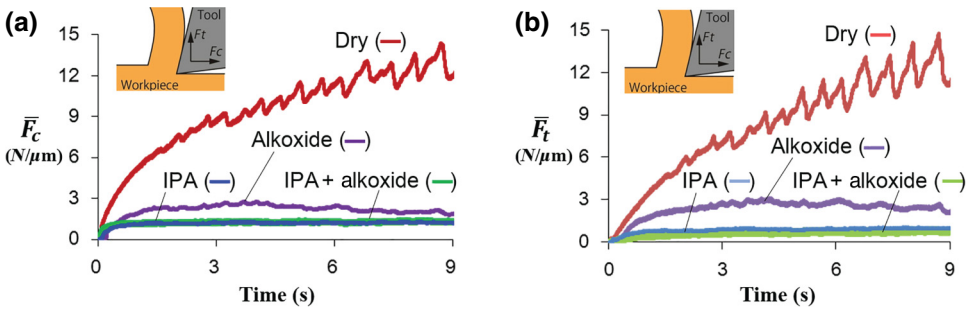

FIG. 10. The specific force ($\bar{F} = F/h_0$) in shear deformation under various cutting conditions (dry, IPA, and alkoxide). (a) The specific cutting force ($\bar{F}_c$) and (b) the specific thrust force ($\bar{F}_t$). $\bar{F}_c$ and $\bar{F}_t$ in IPA cutting are smaller by an order of magnitude compared to dry cutting, whereas the specific forces in alkoxide cutting are smaller by a factor of 6 relative to dry cutting. The specific forces in that case of IPA + alkoxide cutting are identical to those with IPA cutting.

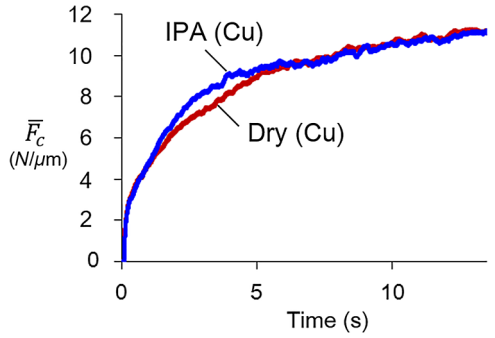

FIG. 11. The specific cutting force in annealed Cu for dry and IPA cutting ($\alpha = 0°$, $h_0 = 50$ μm, $V_0 = 5$ mm/s). In contrast to the Al cutting, IPA has no effect on the cutting force in the Cu. This strongly suggests that the lubrication in the Al is not because of the alcohol itself but is due to the formation of an alkoxide layer along the chip undersurface.

In order to better demonstrate the uniqueness of this configuration, two additional secondary experiments are carried out.

1. Lubrication due to alkoxide film

To emphasize the important role of the alkoxide film in effecting lubrication of the chip-tool interface, annealed Cu is cut under identical conditions to those described in Sec. III for Al. It has been shown previously that the cutting characteristics of annealed Cu in dry cutting are very similar to those of Al under similar conditions: a sinuous-flow mode prevails, with a very thick chip and a large cutting force [10,11].

Importantly, there is no report of any alkoxide-type layer occurring on freshly generated Cu surfaces. Therefore, any change in F_c with Cu, if observed, can only be attributed to the presence of an IPA liquid film, devoid of alkoxide, in the tool-chip contact. Figure 11 shows the variation of F_c in dry and IPA cutting of annealed Cu. The force is essentially the same in both cases, which indicates that the lubricating effect of the IPA, without the alkoxide layer at the tool-chip interface, is negligible. Furthermore, it unambiguously points to the alkoxide layer as the cause of the large reduction in friction observed in aluminum IPA cutting (Sec. D).

Taken together, these results establish the key role of the alkoxide in reducing the friction force (drag) at the tool-chip contact when cutting Al. Equally importantly, this drag reduction alters the flow mode in the primary deformation zone: the sinuous flow of dry cutting is replaced by a laminar flow mode in IPA cutting, with much smaller forces and less energy consumption, and deformation strains. These latter attributes are also highly desirable in practice.

2. The importance of the initial oxide layer

The alkoxide-cutting experiments establish that the deformation can be influenced not just by alkoxide being present at the tool-chip interface, as in the IPA-cutting experiments, but also when it is present at the chip free surface. This result leads to a hypothesis about the influence of the free surface in the IPA-cutting experiment. Since the experiment is conducted in a medium of IPA, it is present at both the chip free surface and the tool-chip interface and possibly influences the deformation from both surfaces. In order to exclude this possibility, the following secondary experiment is performed. An annealed Al workpiece, with natural surface oxide layer present, is immersed in IPA for 10 min at room temperature and then allowed to air-dry completely by evaporation. Any possible reaction with the workpiece free surface should have occurred at this time and so should influence subsequent deformation. This Al workpiece is then cut in the dry condition without application of IPA. Sinuous flow with a thick chip results, with an $F_c \simeq 450$ N; indistinguishable from the previous Al dry cutting (see Fig. 10). This shows that the initial IPA application does not result in any alkoxide formation on the workpiece. This is as expected, since the inherent oxide layer on the Al surface would prevent any chemical reaction with the alcohol. Therefore, in the case of IPA cutting, the formation of the alkoxide is solely restricted to the tool-chip interface and the newly created (cut) workpiece surface; the free surface of the chip is chemically unaltered. Furthermore, the alkoxide is formed only when fresh Al is exposed to the alcohol by the cutting. This result validates the hypothesis that the results of the IPA-cutting experiment are purely due to lubrication at the tool-chip interface due to the presence of the alkoxide.

F. Surface quality

The three flow modes—sinuous, laminar, and segmentation—observed in the dry-, IPA-, and alkoxide-cutting experiments, respectively, also show characteristic features on the macroscale. The most notable of these signatures are the forces and energy dissipation, just discussed, and the quality of the final cut surface.

The quality of the cut surface is of interest from an applications standpoint, as it determines component performance. The requirements on this surface usually include minimal density of defects such as cracks and tears and small values of roughness. The three ambient conditions, with distinct flow modes and force levels, give rise to surfaces with distinctly different properties.

Sinuous flow with folding, typical of dry cutting, results in a surface of poor quality [Fig. 12(a)]. Optical profilometry of the cut surface for this flow condition reveals large tears and/or cracks; an example of such a tear is shown in Fig. 12(a). Each of these tears often spans the entire width

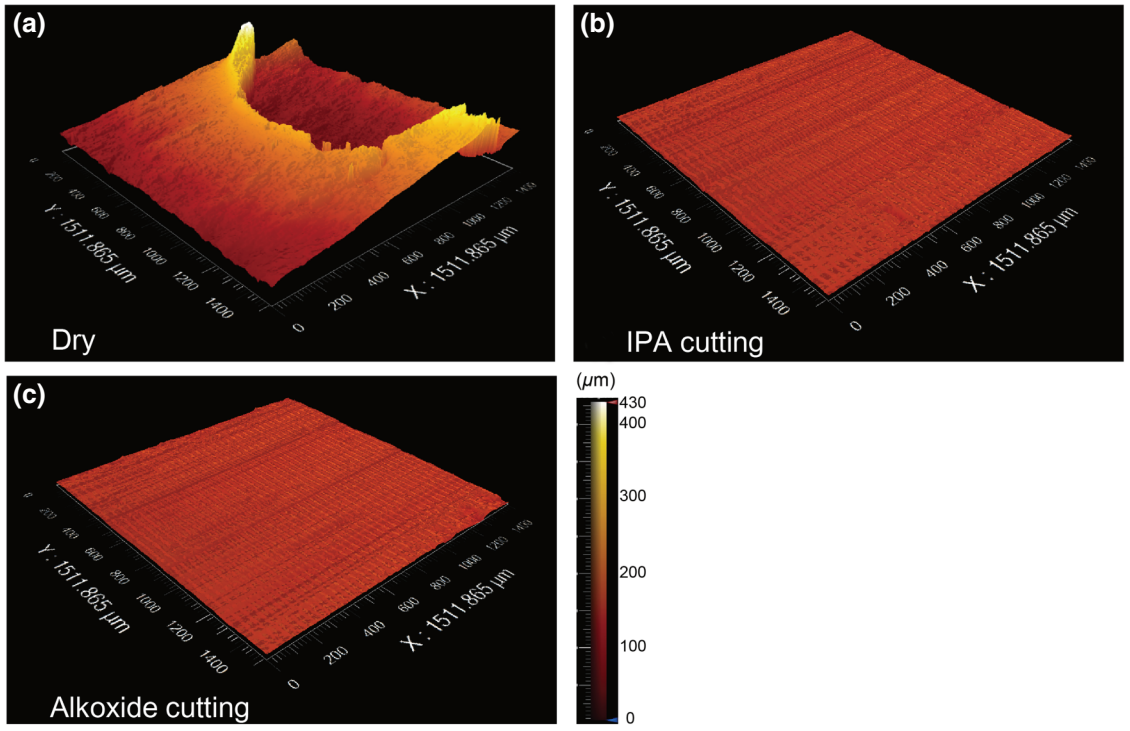

FIG. 12. Three-dimensional optical profilometer images of the cut surface of Al, showing the topography and defect features. (a) Dry cutting: a surface defect in the form of a tear is seen. (b),(c) In the case of IPA and alkoxide cutting, the quality of the cut surface is seen to be much better, with a relatively smooth surface topography and the absence of defects such as tears.

of the cut. By examining large regions of the cut surface, the tears are estimated to occur at an average frequency of 0.3 per mm. This spacing is consistent with the oscillation frequency of the forces in dry cutting (see Fig. 10). The average depth of the tears (peak to valley distance) is about 430 μm, which is much greater than h_0. While the mechanism of formation of these tears has not yet been resolved, it has been shown in a related sliding configuration [27] that the folds arising in sinuous flow nucleate defects by various types of fold-splitting in the wake of the tool or die. We envisage a similar mechanism herein, also accentuated by high F_f, in the sinuous-flow mode, which inhibits easy flow of the chip against the tool face. No dead-metal or stagnation zones are observed on the tool rake face, thereby ruling them out as potential causes for the tears and cracks.

In sharp contrast to dry cutting, both IPA cutting with laminar flow and alkoxide cutting with segmented flow result in much smoother cut surfaces [see Figs. 12(b) and 12(c)]. First, there are very few, if any, tears and cracks on the surface. Second, the surface roughness values, R_a, are 1.75 and 1.80 μm for the IPA and alkoxide cutting, respectively. The peak-to-valley distances are measured to be 8.1 and 6.0 μm, respectively. The improvement in the finish, when compared to dry cutting, is more than an order of magnitude, even simply by comparing the peak-to-valley distance. This significant improvement in quality is undoubtedly a consequence of the corresponding flow modes, with resulting (much) smaller forces (Fig. 10).

V. DISCUSSION

The high-speed *in situ* measurements in large-strain deformation of Al in the presence of isopropyl alcohol (IPA) reveal an intricate link between surface-plastic-flow modes and the surrounding chemical environment. Based on the conditions (dry, IPA, alkoxide or IPA + alkoxide cutting), three distinct flow modes are produced in the same system without changing the workpiece material or deformation geometry. Transitions between the flow modes occur purely due to a change in the chemical environment. These flow transitions are accompanied by large-scale changes in the cutting forces, energy, and deformation strain, as well as quantifiable changes in the properties of the cut surface. The occurrence of different flow modes is principally determined by the specific manner in which the IPA reacts with the Al surface—the formation of an alkoxide film on the tool-chip interface *vis-à-vis* the workpiece free surface results in two completely different flow modes. In this context, the present mechanochemical effect is distinct from our recent report of a material-independent mechanochemical effect in metals [28]. In the latter case, a single flow transition—from

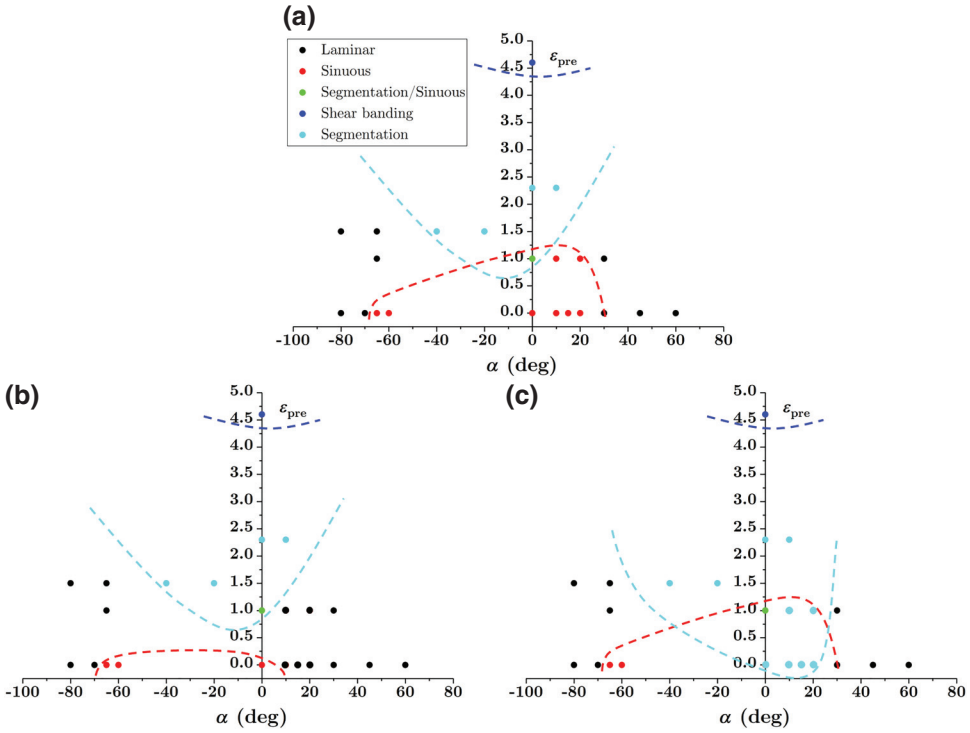

FIG. 13. A phase diagram showing the stability domains of different plastic-flow modes. A point on this diagram corresponds to a single experiment specified by the deformation geometry (rake angle α) and the initial deformation state (prestrain, ϵ_{pre}) of the workpiece surface. (a) A phase diagram for dry cutting (no chemical environment), showing points with sinuous flow (red), laminar flow (black), segmented flow (cyan), and shear banding (blue). The buckling (red) and crack-initiation (cyan) curves are also shown. (b) During IPA cutting, the buckling curve shifts downward due to lubrication by the alkoxide layer: this causes a flow transition from sinuous to laminar. (c) In the case of alkoxide cutting, the crack-initiation curve shifts downward, resulting in a transition from sinuous to segmented flow.

sinuous to segmented—was observed with a range of chemical media and with three different metal systems, the prerequisite being strong adhesion of the chemical medium to the metal surface [28]. The present results from the Al-IPA system highlight a mechanochemical effect that is material and chemical medium specific. The effect demonstrates a wider range of flow transitions, therefore, enabling one to more fundamentally probe the stability of plastic flow in large-strain deformation as discussed below.

A. Flow stability, plastic buckling, and fracture

The role of stability in determining the deformation mode is clearly exemplified in the case of sinuous flow. As shown in Sec. A, this flow is initiated by a plastic buckling event on the workpiece surface just ahead of the tool or chip, leading to material folding. The buckling instability can be understood using a simplified model of a beam on a foundation representing the undeformed chip material ahead of the tool [11,33]. Consequently, by considering the competition between material removal by homogeneous laminar flow and plastic deformation via buckling, the onset of sinuous flow can be predicted as a function of α and initial material prestrain ϵ_{pre}. When buckling occurs, laminar flow becomes unstable and sinuous flow results.

Sinuous flow itself can become unstable in the presence of certain adsorptive chemicals at the free surface of the chip. In the case of alkoxide cutting, the presence of alkoxide on the uncut Al workpiece surface (Fig. 3) alters the flow from sinuous to segmented (Sec. C). Segmentation is characterized by periodic and repeated cracks propagating from the chip free surface toward the tool tip (Fig. 9). Usually, segmentation is observed in metals that are relatively less ductile, when the plastic strain at the chip free surface reaches a critical value [38]. However, when segmentation is observed in annealed Al, it being a prototypical example of a highly ductile metal, there is a need for an alternative explanation.

The sudden transition from ductile to brittle behavior is reminiscent of the stress-corrosion cracking and hydrogen embrittlement that is reported in structural metals, usually with disastrous consequences ensuing [16–18]. In alkoxide cutting, it is likely that the chemically adsorbed alkoxide layer effectively decreases the surface energy of the workpiece; such a decrease can lead to local embrittlement of the metal, in line with theoretical predictions [21,53].

In addition to the surface-energy reduction, the presence of notchlike features at the surface can create an environment conducive for crack propagation. Figure 6 shows how the development of the initial buckle between two pinning points in sinuous flow leads to the formation of such features. In the presence of the alkoxide layer, a notch tip corresponding to one pinning point becomes unstable to crack growth as opposed to continued plastic deformation. Consequently, the propagation of cracks from the pinning points makes sinuous flow an unstable flow mode and leads, instead, to segmented flow, as seen in Fig. 9. This type of transition is also a signature of a material-independent mechanochemical effect, wherein surface-energy reduction via physical adsorption, coupled with preexisting notchlike features on the surface, can drive crack growth [28].

On the other hand, the IPA-cutting experiment (Sec. B) provides evidence for an alternate route to alter stability of sinuous flow—if the forces at the tool-chip interface are reduced by the use of a suitable lubricating film, the compressive loading imposed on the plastic zone ahead of the chip also reduces. This indeed occurs with IPA cutting, wherein the cutting and thrust forces are both reduced by an order of magnitude (Fig. 10). As a result, the buckling threshold force is shifted (increased) so that laminar flow becomes the more stable mode. Consequently, the metal demonstrates homogeneous laminar flow (Fig. 7). Here, the alkoxide layer at the tool-chip interface plays the role of the lubricating film.

In summary, sinuous flow transitions into laminar flow when the tool-chip interface is lubricated and to segmented flow when a suitable chemical is adsorbed on the chip free surface. Both of these flow modes are characterized by much smaller forces and energy dissipation *vis-à-vis* sinuous flow. Furthermore, in the presence of both these conditions, i.e., tool-chip interface lubrication and an adsorbed layer on the free surface, the development of plastic buckling with folding is again prevented. Consequently, the notches necessary for a crack to propagate do not develop. Therefore, although the metal free-surface energy might be altered due to the alkoxide, the absence of notchlike features on the surface precludes the possibility of crack propagation and segmented flow. This is confirmed experimentally by performing alkoxide cutting in the presence of IPA, so that the alkoxide is present on both the free surface as well as the tool-chip interface. The resulting flow is laminar, with no signs of any crack growth events.

B. A phase diagram for stability of surface plastic flow

The observations can now be presented in the form of a stability diagram for surface-plastic-flow modes [see Fig. 13(a)]. Here, the vertical axis is the initial prestrain (ϵ_{pre}) in the workpiece and the horizontal axis is the deformation geometry (rake angle α). This figure represents a "phase diagram" in that each point in the $\epsilon_{\text{pre}} - \alpha$ plane corresponds to one particular experimental condition, i.e., a specific prestrain and geometry. In the absence of any plastic instabilities, the default flow mode, for any $\epsilon_{\text{pre}}, \alpha$ is one of homogeneous strain, i.e., laminar flow (black circle). This figure also includes negative values for α, with very large negative values corresponding to sliding without any chip formation.

The plastic-buckling instability, leading to sinuous flow, can be incorporated into this diagram by using a simple model [33]. As a result, a critical $\epsilon_{\text{pre}}(\alpha)$ relation is obtained—the red dashed curve in Fig. 13(a). For ϵ_{pre} values that lie below this curve, the material buckles prior to laminar flow so that folding with sinuous flow ensues. This region of the $\epsilon_{\text{pre}} - \alpha$ diagram corresponds to situations where sinuous flow is the stable flow mode. Similarly, for α values above this curve, the cutting forces are sufficiently small that plastic buckling no longer occurs. In this region, laminar flow predominates, as is well known [13,33].

On the other hand, segmented flow can be incorporated into the phase diagram by considering the threshold for crack nucleation from the chip free surface. This curve [cyan in Fig. 13(a)] has the following characteristics, as derived from prior work [38]. Crack initiation is usually favored in regions of high accumulated plastic strain. However, for large positive α, the amount of prestrain required for crack initiation is quite large and under these conditions only laminar flow occurs. For less positive α, the ϵ_{pre} required for crack initiation is smaller, implying an increased propensity for segmented flow. Consequently, the area of the phase diagram above the cyan curve corresponds to segmented flow—the experimental points (cyan circles) support this observation.

Finally, for completeness, the condition for shear-band flow is also depicted (blue circle). Shear banding is a mode of flow localization and is typical at very high ϵ_{pre} (>4.5). The mechanics of shear-band formation is, however, outside the scope of the present study and is discussed elsewhere [12,54]

The stability phase diagram provides a basis for explaining the observed flow transitions:

(1) *IPA cutting*: Under these conditions, a lubricating film is present at the tool-chip interface. This film significantly reduces the propensity for plastic buckling, resulting in a transition from sinuous to laminar flow. Consequently, in Fig. 13, the buckling curve is shifted downward (red dashed line) [see Fig. 13(b)]. Now, points that initially result in sinuous flow (red circles) switch stability to laminar flow (black circles).

(2) *Alkoxide cutting*: In the presence of an alkoxide surface film, the workpiece surface energy is lowered. Correspondingly in Fig. 13(c), the crack nucleation threshold curve (cyan) is shifted downward. In this case, even though plastic buckling is more stable than laminar flow,

crack nucleation at pinning points represents an alternative stable mode. As a result, cracks now grow from the pinning points toward the tool tip, leading to periodic segmentation (Fig. 9). Consequently, points that otherwise show sinuous flow (red circles, part (a)) now demonstrate segmented flow (cyan circles) under identical ϵ_{pre}-α conditions.

The schematic diagram qualitatively explains the observations for a given initial starting condition. The same starting conditions in Figs. 13(a) switch stability in parts 13(b) and 13(c) due to changes in the buckling or crack-initiation thresholds. However, additional experimental validation is necessary to establish the plastic buckling (red) and crack-initiation (cyan) curves more quantitatively. This will involve further probing of the ϵ_{pre}-α space by performing a series of experiments with varying initial conditions. Furthermore, the diagram is likely to change depending on the material chosen (Al vs Cu, for instance) and will have to be recomputed accordingly. However, this process can be accelerated by noting that *ex situ* or macroscale observations such as forces can distinguish certain flow modes (see Fig. 10), precluding the need for detailed *in situ* flow mapping.

C. Implications for processing applications

Fundamentally, the results show that surface plastic flow in large-strain shear deformation can be varied by suitable modification of the chemical environment, suggesting routes for improving performance of machining and surface-deformation processes. In particular, the observations strongly suggest that the chemical ambient environment in the deformation zone can be a useful variable for process control, over and beyond the usual process variables such as the deformation geometry and the workpiece initial deformation state. From a technological standpoint, the results have two immediate implications. First, the machining of many soft metals and/or highly strain-hardening metals (e.g., Al, Cu, Fe, Ni, Ta, and stainless steels), notoriously referred to as being gummy and difficult to cut, could potentially be improved manyfold by the use of a suitable chemical (or corrosive) effect either at the chip undersurface or at the workpiece free surface. For this purpose, the medium must be designed or tailored to effect a chemical reaction at one or more of these surfaces and interfaces. The improvement in process performance is reflected in significantly reduced forces and energy dissipation (cf., Fig. 10), and improved surface quality (cf., Fig. 12). The reduced specific energy will also result in lower temperatures in the deformation zone, with additional benefits to workpiece surface quality and tool wear. Second, the chemical medium can be tailored to the metal, via its effect on the initial workpiece surface, as is demonstrated in alkoxide cutting. In many machining, surface-generation, and forming processes, the workpiece free surfaces are quite readily accessed by the chemical media; whereas lubrication of the tool- or die-workpiece contact is much more difficult due to limits imposed by the intimate and severe nature of this contact, a consequence of large contact pressures and elevated temperatures imposed by the tool. In fact, such surface phenomena are already beginning to find use for improved efficiency in material processing [55]. Thus attractive possibilities exist for a class of mechanochemically assisted cutting and deformation processes for metals, akin to those developed for nonmetals, that exploit surface chemistry principles.

The results also have scientific implications. First, the use of chemical media may provide a route for studying the surface-plastic-flow modes and stability of this plastic flow systematically. Second, it points to critical areas where current modeling of large-strain deformation in metal-cutting and deformation processes needs improvement. One of these is the friction boundary condition at the tool-chip contact in lubricated cutting. The IPA-cutting results conclusively show that this boundary condition cannot just be described via the use of a Coulomb-type friction coefficient, with a smaller value than in dry cutting, as is often done. The other critical area pertains to incorporating flow-stability criteria (e.g., buckling and segmentation) and microstructure in continuum models of metal cutting. This criterion is necessary to predict unsteady flow modes such as sinuous and segmented flows and the flow ransitions that have been demonstrated. Lastly, the mechanochemical effect highlighted herein is intriguing in that its manifestation is coupled to the occurrence of unsteady flow modes such as sinuous flow in metals. We plan to elaborate on some of these topics and questions in future work.

VI. CONCLUSIONS

A study is made of the development of surface plastic flow in large-strain deformation of metals in the presence of a chemically active medium. Using high-speed *in situ* imaging observations of simple-shear deformation in a model system—plane-strain cutting of soft annealed aluminum in an isopropyl alcohol (IPA) environment—the occurrence of three distinct plastic-flow modes is demonstrated. All of these flow modes are manifest in the same material depending on the details of the IPA application, under otherwise identical conditions of deformation geometry and initial workpiece state (annealed). Transitions between these modes are effected by the nature of the chemical environment—a mechanochemical effect.

In dry cutting, in the absence of the chemical medium, the flow mode is (nonlaminar) sinuous flow characterized by surface plastic buckling and large-amplitude folding. The corresponding strain field is highly nonhomogeneous

with large deformation strains and very high forces, even though the material being sheared is quite soft. However, when the shear deformation is imposed in the presence of the IPA, two fundamentally distinct plastic-flow modes are seen—segmented flow distinguished by crack propagation from the free surface of the metal (chip free surface) and nonhomogeneous straining; and laminar flow with a smooth homogeneous strain field. Both of these flow modes are characterized by small deformation (cutting) forces and specific energy—almost an order of magnitude smaller than with sinuous flow—effected by reduced straining. The change in flow mode in the presence of the IPA is shown to result from the reaction between the IPA and freshly generated Al surfaces, the latter a product of the deformation. When the IPA application is tailored to create an alkoxide layer on the workpiece free surface ahead of the tool, the ductility of the surface layer is lowered—local embrittlement—with periodic crack nucleation and propagation from this surface resulting in the segmented flow. In contrast, when the IPA action is tailored to create a highly effective lubricant film (most likely an alkoxide layer) on the chip undersurface in the tool-chip contact region, the resulting lowering of the imposed forces suppresses plastic buckling and sinuous flow. Instead, laminar flow, with much smaller deformation strains, results. The mechanochemical effect highlighted herein is shown to be strongly coupled to the nucleation of sinuous flow, distinguishing it from other flow and fracture phenomena in surface plasticity such as liquid metal embrittlement and stress corrosion cracking.

The occurrence of different flow modes and flow transitions and the coupling between the mechanochemical effect and sinuous flow are explained in the framework of plastic-flow stability. In this framework, the stability boundaries are altered by the action of the chemical medium on the metal surface, thereby creating conditions for crack nucleation or establishing laminar flow. The work suggests interesting opportunities, exploiting the mechanochemical effect, for much improved cutting of soft and highly strain-hardening metals such as copper, iron, nickel, and stainless steels— materials often termed "gummy" because of the difficulty involved in their cutting.

ACKNOWLEDGMENTS

The authors would like to acknowledge support from NSF Grants No. CMMI 1562470 and DMR 1610094. A.U. and T.S. contributed equally to this work.

[1] C. Zener*Fracturing of Metals* (American Society for Metals, Cleveland, Ohio, 1948), p. 3.
[2] R. Hill, The mechanics of machining: A new approach, J. Mech. Phys. Solids **3**, 47 (1954).
[3] J. R. Rice, in *Proceedings of the 14th International Congress on Theoretical and Applied Mechanics*, edited by W. T. Koiter (North-Holland, Amsterdam, 1976), p. 207.
[4] P. Dewhurst, On the non-uniqueness of the machining process, Proc. R. Soc. London A: Math. Phys. Eng. Sci. **360**, 587 (1978).
[5] R. F. Recht, Catastrophic thermoplastic shear, J. Appl. Mech. **31**, 189 (1964).
[6] J. G. Ramsay, and M. I. Huber, *Modern Structural Geology, Volume 2: Folds and Fractures* (Academic Press, London, 1987).
[7] T. J. Burns, and M. A. Davies, Nonlinear Dynamics Model for Chip Segmentation in Machining, Phys. Rev. Lett. **79**, 447 (1997).
[8] B. Dodd, S. M. Walley, R. Yang, and V. F. Nesterenko, Major steps in the discovery of adiabatic shear bands, Metall. Mater. Trans. A **46**, 4454 (2015).
[9] L. Dai, M. Yan, L. Liu, and Y. Bai, Adiabatic shear banding instability in bulk metallic glasses, Appl. Phys. Lett. **87**, 141916 (2005).
[10] H. Yeung, K. Viswanathan, W. D. Compton, and S. Chandrasekar, Sinuous flow in metals, Proc. Natl. Acad. Sci. **112**, 9828 (2015).
[11] H. Yeung, K. Viswanathan, A. Udupa, A. Mahato, and S. Chandrasekar, Sinuous Flow in Cutting of Metals, Phys. Rev. Appl. **8**, 054044 (2017).
[12] K. Viswanathan, A. Udupa, H. Yeung, D. Sagapuram, J. B. Mann, M. Saei, and S. Chandrasekar, On the stability of plastic flow in cutting of metals, CIRP Ann.-Manuf. Technol. **66**, 69 (2017).
[13] M. C. Shaw, *Metal Cutting Principles* (Oxford University Press, New York, 2005).
[14] F. P. Bowden, and D. Tabor, *Friction: An Introduction to Tribology* (RE Krieger Publishing Company, New York, 1973).
[15] R. M. Latanision, and R. H. Jones, *Chemistry and Physics of Fracture* (Martinus Nijhoff Publishers, Dordrecht, 1987).
[16] W. Rostoker, J. McCaughey, and H. Markus, *Embrittlement by Liquid Metals* (Reinhold Pub. Corp., New York, 1960).
[17] W. D. Robertson, *Stress Corrosion Cracking and Embrittlement* (J. Wiley, New York, 1956).
[18] O. Reynolds, Chem. News **29**, 117 (1874); mem, Proc. Literary Philos. Soc. Manchester **13**, 93 (1874).
[19] P. Rehbinder, New physico-chemical phenomena in the deformation and mechanical treatment of solids, Nature **159**, 866 (1947).
[20] E. D. Shchukin, The influence of surface-active media on the mechanical properties of materials, Adv. Colloid Interface Sci. **123**, 33 (2006).
[21] J. R. Rice, in *Chemistry and Physics of Fracture*, edited by R. M. Latanision and R. H. Jones (Martinus Nijhoff, Boston, 1987), p. 23.
[22] R. M. Latanision, in *Surface Effects in Crystal Plasticity*, edited by R. M. Latanision and J. T. Fourie (Nordhoff, Leyden, 1977), p. 3.
[23] A. R. C. Westwood, and J. J. Mills, in *Surface Effects in Crystal Plasticity*, edited by R. M. Latanision and J. T. Fourie (Nordhoff, Leyden, 1977), p. 835. See also discussion by A. Argon, following the article.
[24] N. P. Suh, The delamination theory of wear, Wear **25**, 111 (1973).

[25] K. Johnson, Contact mechanics and the wear of metals, Wear **190**, 162 (1995).
[26] J. M. Challen, L. J. McLean, and P. L. B. Oxley, Plastic deformation of a metal surface in sliding contact with a hard wedge: Its relation to friction and wear, Proc. R. Soc. London A: Math. Phys. Eng. Sci. **394**, 161 (1984).
[27] A. Mahato, Y. Guo, N. K. Sundaram, and S. Chandrasekar, Surface folding in metals: A mechanism for delamination wear in sliding, Proc. R. Soc. A **470**, 20140297 (2014).
[28] A. Udupa, K. Viswanathan, M. Saei, J. B. Mann, and S. Chandrasekar, Material-Independent Mechanochemical Effect in the Deformation of Highly-Strain-Hardening Metals, Phys. Rev. Appl. **10**, 014009 (2018).
[29] P. A. Rehbinder, and E. D. Shchukin, Surface phenomena in solids during deformation and fracture processes, Prog. Surf. Sci. **3**, 97 (1972).
[30] K. H. Brown, D. A. Grose, R. C. Lange, T. H. Ning, and P. A. Totta, Advancing the state of the art in high-performance logic and array technology, IBM J. Res. Dev. **36**, 821 (1992).
[31] Y. Namba, and H. Tsuwa, Mechanism and some applications of ultra-fine finishing, CIRP Ann.-Manuf. Technol. **27**, 511 (1978).
[32] M. Krishnan, J. W. Nalaskowski, and L. M. Cook, Chemical mechanical planarization: Slurry chemistry, materials, and mechanisms, Chem. Rev. **110**, 178 (2009).
[33] A. Udupa, K. Viswanathan, Y. Ho, and S. Chandrasekar, The cutting of metals via plastic buckling, Proc. R. Soc. A **473**, 20160863 (2017).
[34] M. E. Merchant, Mechanics of the metal cutting process. I. Orthogonal cutting and a type 2 chip, J. Appl. Phys. **16**, 267 (1945).
[35] R. Komanduri, and B. Von Turkovich, New observations on the mechanism of chip formation when machining titanium alloys, Wear **69**, 179 (1981).
[36] K. Nakayama, in *Proceedings of International Conference on Production Engineering* (1974), p. 572.
[37] W. A. Backofen, Deformation processing, Metall. Trans. **4**, 2679 (1973).
[38] Y. Guo, W. D. Compton, and S. Chandrasekar, *In situ* analysis of flow dynamics and deformation fields in cutting and sliding of metals, Proc. R. Soc. A **471**, 20150194 (2015).
[39] A. R. C. Westwood, Tewksbury lecture: Control and application of environment-sensitive fracture processes, J. Mater. Sci. **9**, 1871 (1974).
[40] K. Dao, and D. Shockey, A method for measuring shear-band temperatures, J. Appl. Phys. **50**, 8244 (1979).
[41] D. Bradley, Metal alkoxides, Prog. Inorg. Chem. 2, 303 (1960).
[42] O. Helmboldt, L. Keith Hudson, C. Misra, K. Wefers, W. Heck, H. Stark, and M. Danner, in *Ullmann's Encyclopedia of Industrial Chemistry* (Wiley-VCH Verlag GmbH & Co. KGaA, 2000), p. 578.
[43] J. Gladstone, and A. Tribe, I. Aluminium alcohols. Part I. Their preparation by means of the aluminium-iodine reaction, J. Chem. Soc. Trans. **39**, 1 (1881).
[44] R. Montgomery, The effect of alcohols and ethers on the wear behavior of aluminum, Wear **8**, 466 (1965).
[45] M. C. Shaw, Action of *n*-primary alcohols as metal cutting fluids alternating properties with chain length, J. Am. Chem. Soc. **66**, 2057 (1944).
[46] S. Hironaka, and T. Sakurai, The effect of pentaerythritol partial ester on the wear of aluminum, Wear **50**, 105 (1978).
[47] F. P. Bowden, and D. Tabor, *The Friction and Lubrication of Solids* (Clarendon Press, Oxford, 2001).
[48] C. Kajdas, About an anionic-radical concept of the lubrication mechanism of alcohols, Wear **116**, 167 (1987).
[49] J. E. Williams, E. F. Smart, and D. R. Milner, Metallurgy of machining. Part 1: Basic considerations and the cutting of pure metals, Metallurgia **81**, 3 (1970).
[50] V. Piispanen, Theory of formation of metal chips, J. Appl. Phys. **19**, 876 (1948).
[51] E. Lee, and B. Shaffer, The theory of plasticity applied to a problem of machining, J. Appl. Mech. **18**, 405 (1951).
[52] K. Strawhecker, D. Asay, J. McKinney, and S. Kim, Reduction of adhesion and friction of silicon oxide surface in the presence of *n*-propanol vapor in the gas phase, Tribol. Lett. **19**, 17 (2005).
[53] J. R. Rice, and R. Thomson, Ductile versus brittle behaviour of crystals, Philos. Mag. **29**, 73 (1974).
[54] D. Sagapuram, K. Viswanathan, A. Mahato, N. K. Sundaram, R. M'Saoubi, K. P. Trumble, and S. Chandrasekar, Geometric flow control of shear bands by suppression of viscous sliding, Proc. R. Soc. A **472**, 20160167 (2016).
[55] T. Sugihara, Y. Nishimoto, and T. Enomoto, On-machine tool resharpening process for dry machining of aluminum alloys employing lme phenomenon, Precis. Eng. **40**, 241 (2015).